Original Research

Lack of Vitamin D Receptor Causes Dysbiosis and Changes the Functions of the Murine Intestinal Microbiome

Dapeng Jin, MS[1]; Shaoping Wu, PhD[1]; Yong-guo Zhang, PhD[1]; Rong Lu, PhD[1]; Yinglin Xia, PhD[2]; Hui Dong, PhD[3]; and Jun Sun, PhD[1]

[1]Department of Biochemistry, Rush University Medical Center, Chicago, Illinois; [2]Department of Biostatistics and Computational Biology, University of Rochester, Rochester, New York; and [3]Department of Gastroenterology, Xingqiao Hospital, The Third Military Medical University, Chongqing, China

ABSTRACT

Purpose: The microbiome modulates numerous aspects of human physiology and is a crucial factor in the development of various human diseases. Vitamin D deficiency and downregulation of the vitamin D receptor (VDR) are also associated with the pathogenesis of diseases such as inflammatory bowel disease, cancers, obesity, diabetes, and asthma. VDR is a nuclear receptor that regulates the expression of antimicrobial peptides and autophagy regulator ATG16L1. Vitamin D may promote a balanced intestinal microbiome and improve glucose homeostasis in diabetes. However, how VDR regulates microbiome is not well known. In the current study, we hypothesize that VDR status regulates the composition and functions of the intestinal bacterial community.

Methods: Fecal and cecal stool samples were harvested from *Vdr* knockout ($Vdr^{-/-}$) and wild-type mice for bacterial DNA and then sequenced with 454 pyrosequencing. The sequences were denoised and clustered into operational taxonomic units, then queried against the National Center for Biotechnology Information database. Metagenomics were analyzed, and the abundances of genes involved in metabolic pathways were compared by reference to the Kyoto Encyclopedia of Genes and Genomes and Clusters of Orthologous Groups databases.

Findings: In the $Vdr^{-/-}$ mice, *Lactobacillus* was depleted in the fecal stool, whereas *Clostridium* and *Bacteroides* were enriched. Bacterial taxa along the Sphingobacteria-to-Sphingobacteriaceae lineage were enriched, but no genera reached statistical significance. In the cecal stool, *Alistipes* and *Odoribacter* were depleted, and *Eggerthella* was enriched. Notably, all of the taxa upstream of *Eggerthella* remained unchanged. A comparison of $Vdr^{-/-}$ and wild-type samples revealed 40 (26 enriched, 14 depleted) and 72 (41 enriched, 31 depleted) functional modules that were significantly altered in the cecal and fecal microbiomes, respectively (both, $P < 0.05$), due to the loss of Vdr. In addition to phylogenetic differences in gut microbiome with different intestinal origins, we identify several important pathways, such as nucleotide-binding oligomerization domain–like receptor, affected by Vdr status, including amino acid, carbohydrate, and fatty acid synthesis and metabolism, detoxification, infections, signal transduction, and cancer and other diseases.

Implications: Our study fills knowledge gaps by having investigated the microbial profile affected by VDR. Insights from our findings can be exploited to develop novel strategies to treat or prevent various diseases by restoring VDR function and healthy microbe–host interactions. (*Clin Ther.* 2015;37:996–1009)

Accepted for publication April 9, 2015.
http://dx.doi.org/10.1016/j.clinthera.2015.04.004
0149-2918/$ - see front matter

Key words: *Bacteroides*, *Clostridium*, dysbiosis, immunity, inflammation, intestine, microbiome, NOD-like receptor, vitamin D, vitamin D receptor.

INTRODUCTION

Microbial habitats in the human body include the skin surface and the mucosa covering the mouth, pharynx, respiratory tract, urogenital tract, and gut, which accommodate and interact with commensal bacteria to fulfill various physiologic functions.[1] The gastrointestinal tract, in particular, harbors the most abundant microflora (100 trillion). The human genome contains over 23,000 genes; however, it is vastly underestimated if we take the microbiome into consideration, which outnumbers the human cells by an order of magnitude.[2] The symbiotic relationship that coevolves over time bestows humans with functions that do not need to be encoded within their own genomes, or at least not completely,[3] and contributes to interindividual differences.[4,5] The gut microbiome not only has been correlated with disorders such as inflammatory bowel diseases (IBD), obesity, and diabetes[6–8] but has also been shown to have extended effects in other, distant organs, including autism spectrum disorder and Alzheimer disease,[9,10] conditions previously thought irrelevant to gastrointestinal bacteria, thus heralding a new era of microbiome studies.

Vitamin D/vitamin D receptor (VDR) deficiency has been associated with various effects in humans, including higher risks for IBD, including ulcerative colitis and Crohn disease.[11,12] Vitamin D supplementation has been reported to have clinical benefit in reducing IBD occurrence and relapse and in improving outcomes.[12] VDR regulates the expression of cathelicidin antimicrobial peptides (CAMPs), β-defensins, and autophagy regulator ATG16L1[13–15] and therefore possesses some antibiotic properties. For example, [1,25$(OH)_2D_3$] leads to up-regulation of CAMPs and the killing of intracellular *Mycobacterium tuberculosis* in human monocytes.[16] These findings give rise to the inference that vitamin D/VDR signaling may dramatically change the bacterial landscape in the gut. Recent studies have reported that the absence of VDR is associated with shifts in the bacterial load and profile.[15,17] However, an accurate characterization of VDR regulation of the microbiota remains unavailable.

In the present study, we hypothesized that VDR status regulates the composition and functions of the bacterial community in the intestine. We investigated fecal and cecal stool samples from whole-body *Vdr* knockout ($Vdr^{-/-}$) and wild-type (WT) mice, aiming to profile the intestinal microbiomes of animals of different Vdr status. Our study may greatly enrich our understanding of the mechanisms underlying defects caused by VDR deficiency and help us to better navigate therapeutic interventions targeting host–bacteria interactions.

METHODS AND MATERIALS

Statement of Ethics

All animal work was approved by the Committee on Animal Resources, Rush University Medical Center (Chicago, Illinois).

Mice

WT and $Vdr^{-/-}$ C57BL/6 mice (purchased from Jackson Laboratory, Bar Harbor, Maine) were bred as previously described.[18] Tail snips were collected 4 weeks after the mice were born. Littermates 6 to 8 weeks old were chosen from each group and cohoused until the experiments were performed.

Microbial Sampling and Sequencing

The tubes for microbial sampling were autoclaved and then irradiated with ultraviolet light to destroy the contaminating environmental bacterial DNA. The mice were then anesthetized and dissected. Fresh cecal and fecal stools were isolated from the gut and placed into the specially prepared tubes. The samples were kept at low temperature with dry ice and were mailed to the Research and Testing Laboratory for 454 pyrosequencing. The sequences were denoised and subjected to quality checks. Taxonomic identifications were assigned by queries against the National Center for Biotechnology Information database. Initially, 249,435 reads were generated. After denoising, the number was reduced to 173,119, which was then diminished to 160,248 after quality checking. On alignment, 151,543 operational taxonomic units (OTUs) were obtained. For each sample, the number ranged from 1853 to 9264, with a mean of 4736.

454 Pyrosequencing

The V4–V6 region of the samples was amplified for pyrosequencing in the Research and Testing

Laboratory using forward and reverse fusion primers. The forward primer was constructed (5′–3′) with the Roche A linker (CCATCTCATCCCTGCGTGTC TCCGACTCAG), an 8- to 10-bp barcode, and the 530F GTGCCAGCMGCNGCGG primer. The reverse fusion primer was constructed (5′–3′) with a biotin molecule, the Roche B linker (CCTATCCCCT GTGTGCCTTGGCAGTCTCAG), and the 1100R GGGTTNCGNTCGTTR primer (Roche Diagnostics Deutschland GmbH, Mannheim, Germany). Amplifications were performed in 25-μL reaction volumes with Qiagen HotStar Taq master mix (Qiagen Inc, Valencia, California), 1 μL of each primer (5 μmol/L), and 1 μL of template. Reactions were performed on ABI Veriti thermocyclers (Applied Biosytems, Carlsbad, California) under the following thermal profile: 95°C for 5 minutes, then 35 cycles at 94°C for 30 seconds, 54°C for 40 seconds, 72°C for 1 minute, followed by 1 cycle at 72°C for 10 minutes and a 4°C hold. The amplicons were 570 bp in length.

Amplification products were visualized with eGels (Life Technologies, Grand Island, New York). Products were then pooled to equimolar levels, and each pool was cleaned with Diffinity RapidTip (Diffinity Genomics, West Henrietta, New York) and size-selected using Agencourt AMPure XP (Beckman Coulter Inc, Indianapolis, Indiana) after the Roche 454 protocols (454 Life Sciences, Branford, Connecticut). Size-selected pools were then quantified, and 150 ng of DNA was hybridized to Dynabeads M-270 (Life Technologies) to create single-stranded DNA after Roche 454 protocols (454 Life Sciences). Single-stranded DNA was diluted and used in emulsion-based polymerase chain reactions, which were performed and subsequently enriched. Sequencing followed established manufacturer's protocols (454 Life Sciences).

Bioinformatics

Clustering of the reads with 4% divergence on the seed sequences was performed using USEARCH, version 6.0.98 to identify similar clusters.[19] Chimera checking was detected using the de novo method of UCHIIME, version 4.2.40.[20] The sequences were denoised according to a size criterion. For taxonomic identification, the sequences were clustered into OTUs with 0% divergence using USEARCH.[19] The seed sequence was queried against National Center for Biotechnology Information database using a distributed .net algorithm, which makes use of BLASTN+, version 2.2.27 (KrakenBLAST, www.krakenblast.com). Unweighted UniFrac distances were analyzed with the Quantitative Insights Into Microbial Ecology suite software, version 1.9.0 (www.qiime.org) to reflect sample distributions. Alpha and beta diversity, in combination with the metadata, were visualized using the Shannon diversity index, the Chao1 richness index, and principal coordinate analysis (PCoA) plots.[21] Phylotypic Investigation of Communities by Reconstruction of Unobserved States (PICRUSt), version 1.0.0 was used together with HMP Unified Metabolic Analysis Network (HUMAnN), version 0.99[22] for analyzing the metagenomics and to compare the abundances of genes involved in metabolic pathways by reference to the Kyoto Encyclopedia of Genes and Genomes (KEGG)[23] and Clusters of Orthologous Groups[24] databases. Bacterial genomes were imputed according to the similarity of sequenced genomes to reference GreenGenes sequences.[25]

Statistical Analysis

The data are expressed as mean (SD). Differences between 2 samples were analyzed using the *t* test. $P \leq 0.05$ was considered statistically significant. Differences between ≥ 3 groups were analyzed using ANOVA (SAS version 9.2; SAS Institute Inc, Cary, North Carolina).

RESULTS

Effects of Vdr Status and Intestinal Location on the Bacterial Community in the Gut

The OTU data were used for obtaining taxonomic assignments of the microbiomes of the tested samples. On the phylum level, Firmicutes and Bacteroidetes together accounted for a major part of the bacterial population in all samples (90.02%–98.10%). For better differentiation from sample to sample, we present the changes in the intestinal microbiota at the class level, which showed that Bacilli, Clostridia, Erysipelotrichia, Bacteroidia, Actinobacteria, and Verrucomicrobiae topped the list of the most represented classes (92.77%–99.92% combined) (**Figure 1**).

In the $Vdr^{-/-}$ samples, Bacteroidia and Sphingobacteria were enriched, and Bacilli was depleted in the fecal stool, whereas Bacteroidia was depleted in cecal stool. In WT mice, Clostridia were enriched, while Bacteroidia and Flavobacteria were depleted in the

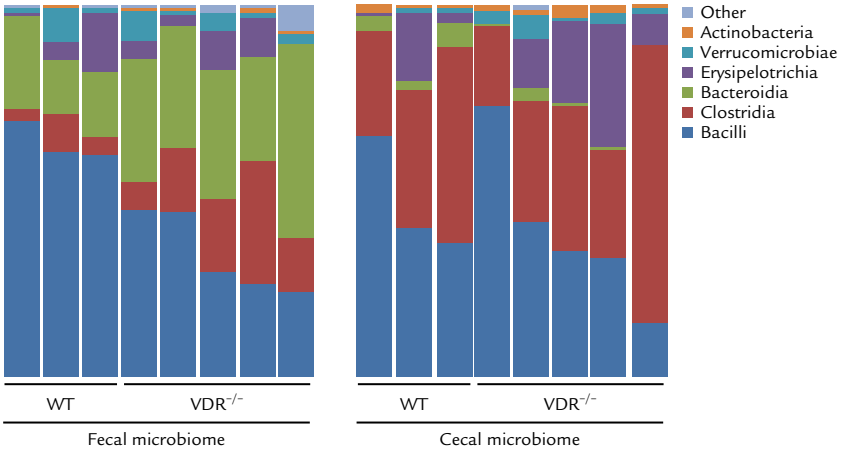

Figure 1. Taxonomic composition of the bacterial community at the class level in stool samples from vitamin D receptor gene knockout (*Vdr*$^{-/-}$) mice (n = 5) and wild-type (WT) mice (n = 3). VDR status and intestinal location were associated with taxonomic alterations of the bacterial community in the gut. Bacilli, Clostridia, Erysipelotrichia, Bacteroidia, Actinobacteria, and Verrucomicrobiae were the most represented bacterial classes.

transition from cecal to fecal stool. Bacteroidia, Flavobacteria, Sphingobacteria, and Cytophagia were depleted in *Vdr*$^{-/-}$ mice in the cecal-to-fecal transition. Vdr status and intestinal location thus altered the bacterial community in the gut. Clearly, Vdr deficiency was associated with dysbiotic changes in the gut.

Microbiome Diversity Indexes of Vdr Statuses

Another crucial criterion of microbial changes is diversity metrics (**Figure 2A and B**), which can be used for assessing the influence of *Vdr* status on microbiome diversity. The Shannon diversity and Chao1 richness indexes suggested both intragroup and intergroup variability in microbial diversity. We also used PCoA to cluster the cecal and fecal microbiomes from *Vdr*$^{-/-}$ and WT mice. The *Vdr*$^{-/-}$ and WT samples clustered independently on the PCoA scale, as did the cecal and fecal samples (**Figure 2C**). Therefore, Vdr status and intestinal location did cause variations in bacterial diversity.

Phylogenetic Differences in the Gut Microbiome, by Vdr Status

In the *Vdr*$^{-/-}$ mice, on the genus level, *Lactobacillus* was depleted in fecal stool, whereas *Clostridium* and *Bacteroides* were enriched (**Figure 3A**). At higher taxonomic levels, Lactobacillales, which includes lactic acid bacteria other than *Lactobacillus,* was also depleted (from 62.71% [4.63%] to 33.23% [10.80%]; $P < 0.01$), indicating a dramatic decrease in the production of lactic acid. The Bacteroidia-to-*Bacteroides* lineage was consistently enriched. Greater than *Clostridium*, the lineage Clostridiaceae was also enriched (from 2.48% [0.81%] to 9.24% [4.58%]; $P < 0.05$). Bacterial taxa were enriched along the Sphingobacteria-to-Sphingobacteriaceae lineage, but no genera reached statistical significance.

In cecal stool, *Alistipes* and *Odoribacter* were depleted, and *Eggerthella* was enriched (**Figure 3B**) in the *Vdr*$^{-/-}$ samples. The lineage from Bacteroidetes to Bacteroidales was depleted in *Vdr*$^{-/-}$ mice, as were the Rikenellaceae-to-*Alistipes* and Peptococcaceae-to-*Odoribacter* lineages. Notably, all the taxa upstream of *Eggerthella* remained unchanged. Compared with the changes in the fecal microbiota, the relative abundance of cecal genera affected by Vdr status was much less.

Taken together, the dramatic reduction of lactic acid bacteria in the fecal microbiome in *Vdr*$^{-/-}$ mice is likely the most important alteration influencing intestinal homeostasis. The fecal microbiome is more severely affected by Vdr status than is the cecal microbiome at the taxonomic level. Taxonomically,

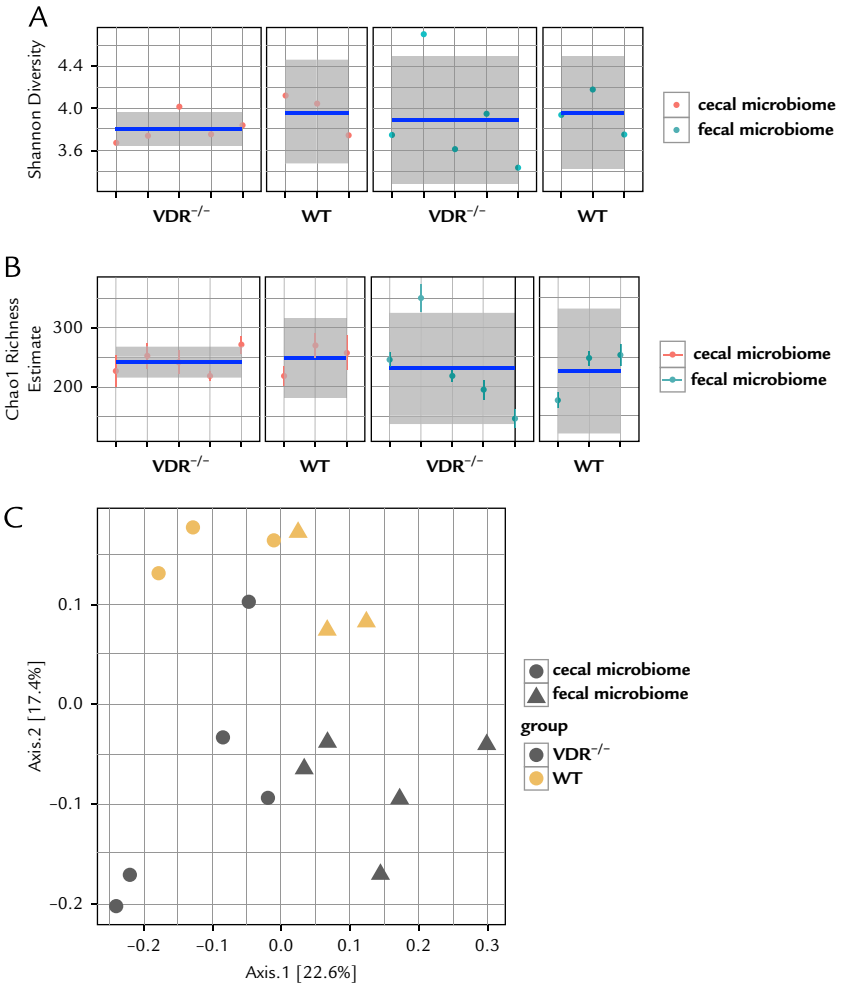

Figure 2. Diversity metrics of the microbiome in fecal and cecal samples from vitamin D receptor gene knockout (*Vdr*$^{-/-}$) mice (n = 5) and wild-type (WT) mice (n = 3). A, Shannon index. B, Chao1 richness index. C, Unweighted UniFrac distances of stool samples from *Vdr*$^{-/-}$ and WT mice on a principal coordinate analysis (PCoA) scale. Shannon index and Chao1 richness reflected variability in microbial diversity within or between groups. The samples were then separated into different clusters on a PCoA scale. cest = cecal contents; dryst = fecal stool; 1 = *Vdr*$^{-/-}$; 2 = WT.

the colon is the major site affected by Vdr status. The Vdr-associated defects in the intestinal microbiome may be related to the weakened capacity of the colon to increase lactic acid bacteria and to contain the growth of *Clostridium* and *Bacteroides*.

Phylogenetic Differences in Gut Microbiomes, by Intestinal Origin

To examine the influences of the intestinal environment on the microbiome, taxonomic alterations between cecal and fecal stool were evaluated. In WT mice, *Clostridium* and *Ruminococcus* were depleted in fecal stool compared with those in the cecal stool, whereas *Tannerella*, *Butyricimonas*, *Bacteroides*, *Alitipes* and *Paraprevotella* were enriched (Figure 4A). In *Vdr*$^{-/-}$ mice, *Lactobacillus* was depleted in fecal stool compared with that in cecal stool, whereas *Tannerella*, *Odoribacter*, *Porphyromonas*, *Butyricimonas*, *Bacteroides*, *Prevotella*, *Rikenella*, *Pedobacter* and *Limibacter* were enriched (Figure 4B). In both the WT and *Vdr*$^{-/-}$ mice, the switch from the cecal to the fecal microbiome was associated with quite diversified

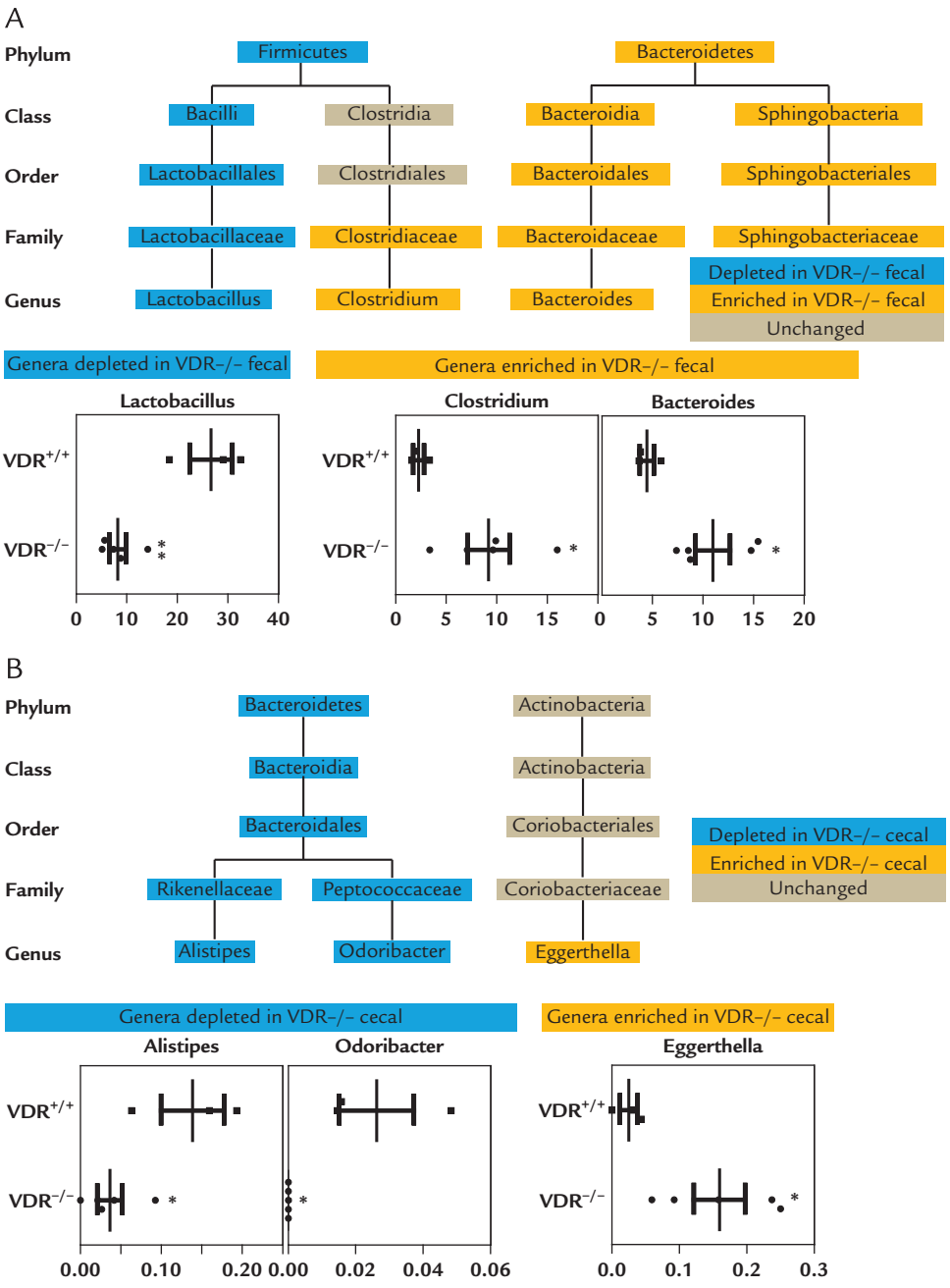

Figure 3. Mean (SD) phylogenetic differences associated with vitamin D receptor gene knockout ($Vdr^{-/-}$). The phylogenetic trees of taxa related to Vdr status and percentages of the affected genera were compared between fecal (A) and cecal (B) contents from $Vdr^{-/-}$ mice (n = 5) and WT mice (n = 3). Only taxa with significantly different abundance or upstream of affected genera were included. Gray denotes statistically unchanged; blue denotes significantly depleted; yellow denotes significantly enriched in $Vdr^{-/-}$ mice. $^{*}P < 0.05$; $^{**}P < 0.01$; $^{***}P < 0.001$.

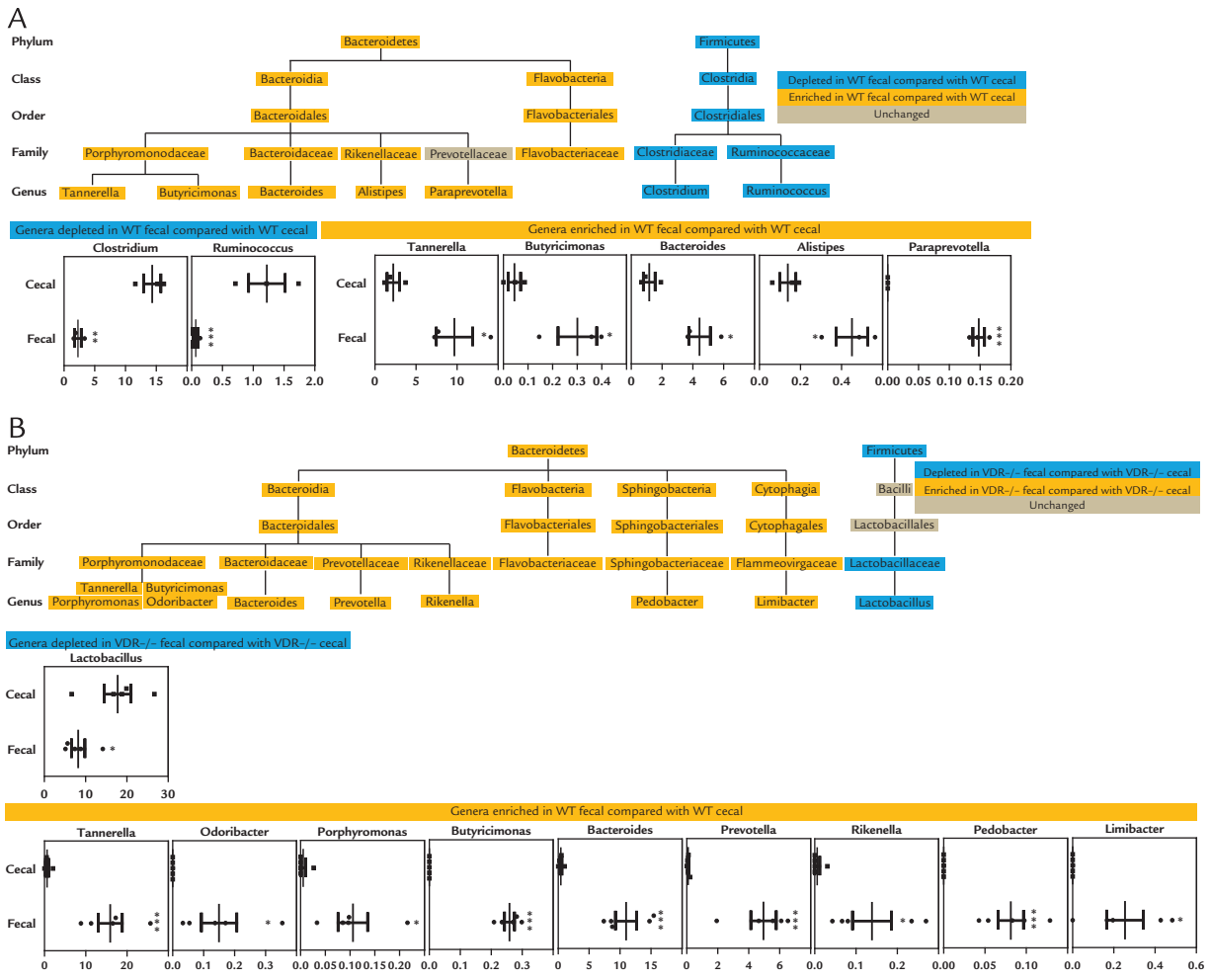

Figure 4. Mean (SD) phylogenetic differences in the transition from the fecal to the cecal microbiome in $Vdr^{-/-}$ mice (n = 5) and WT mice (n = 3). The phylogenetic trees of taxa related to Vdr status and percentages of the affected genera were compared between fecal and cecal microbiome from WT mice (A) and $Vdr^{-/-}$ mice (B). Only taxa with significantly different abundances or that were upstream of affected genera were included. Gray denotes statistically unchanged; blue denotes significantly depleted; yellow denotes significantly enriched in $Vdr^{-/-}$ mice. $^{*}P < 0.05$; $^{**}P < 0.01$; $^{***}P < 0.001$.

changes in taxonomic assignment, which can be ascribed to changes in luminal contents caused by differences in absorption, digestion, fermentation, and secretion. Different sections of the intestinal tract harbor different bacterial communities, which are partially modulated by the host. Among those affected, *Tannerella*, *Butyricimonas,* and *Bacteroides* were similarly enriched in both WT and $Vdr^{-/-}$ mice, indicating a constitutive event in the transition from the cecal to the fecal microbiome, whereas the rest of the affected genera were correlated with Vdr status. The Bacteroidetes-to-Bacteroidales lineage and some of its lower branches, as well as the Bacteroidetes-to-Flavobacteriaceae lineage, were similarly enriched in samples with different Vdr status in the transition from the cecal to the fecal microbiome. What differed was that *Porphyromonas* and *Odoribacter* were also enriched in $Vdr^{-/-}$ mice in the transition from the cecal to the fecal microbiome. In addition, Bacteroidetes-to-*Pedobacter* and Bacteroidetes-to-*Limibacter* lineages were enriched. Finally, instead of depletions of Firmicutes to *Clostridium* and a depletion of Firmicutes to

Ruminococcus, which were seen in the WT mice, there was a depletion of Lactobacillaceae to *Lactobacillus* in the $Vdr^{-/-}$ mice.

Alterations in KEGG Modules of the Gut Microbiome, by Vdr Status

Although the taxonomic assignments revealed interesting findings, functional analyses may prove more meaningful in annotating clinical relevance. With the use of bioinformatics tools, a comparison between $Vdr^{-/-}$ and WT samples revealed 40 (28 enriched, 12 depleted) and 72 (41 enriched, 31 depleted) functional modules that were significantly altered ($P < 0.05$) in the cecal and fecal microbiomes, respectively, due to the loss of Vdr (**Figure 5** and see **Supplemental Tables I–IV** in the online version at http://dx.doi.org/10.1016/j.clinthera.2015.04.004). Several important pathways were likely affected by *Vdr* knockout, including those involved in amino acid, carbohydrate, and fatty acid synthesis and metabolism; detoxification (eg, reduced xylene and dioxin degradation in fecal stool; increased metabolism of drug and xenobiotics by cytochrome P-450 and caprolactam degradation in cecal stool); infections, cancer, and other diseases (eg, increased prion diseases and prostate cancer in fecal stool; increased tuberculosis, renal cell carcinoma, and type II diabetes mellitus in cecal stool); and signal transduction (eg, increased epithelial cell signaling in *Helicobacter pylori* infection in fecal stool; increased peroxisome proliferator-activated receptor, nucleotide-binding oligomerization domain [Nod]–like receptor [Nlr], mitogen-activated protein kinase, and adipocytokine signaling in cecal stool). These data suggest that on *Vdr* knockout, the colon is insulted by more toxins and experiences higher risks for cancer, infections, and other diseases, whereas the effects on the cecum are mainly restricted to the metabolite profile.

Alterations in KEGG Modules of Gut Microbiomes, by Intestinal Origin

We also compared the influence of location on the gut microbiome. As shown in **Supplemental Tables I–IV** (in the online version at http://dx.doi.org/10.1016/j.clinthera.2015.04.004), in $Vdr^{-/-}$ mice, 94 functional modules (66 enriched, 28 depleted) were affected in the fecal compared with the cecal microbiome. In WT mice, 99 functional modules (73 enriched, 26 depleted) were significantly altered in the fecal compared with the cecal microbiome ($P < 0.05$). As shown in **Figure 6A**, in WT mice, with the shift from cecal to fecal microbiome, the affected functional profile involved an extensive increase in metabolite synthesis/metabolism and the enrichment of modules related to diseases such as pertussis, diabetes mellitus, Alzheimer disease, tuberculosis, and renal cell carcinoma and other cancers, as well as decreases in modules involved in bacterial growth, proliferation, and motility, including transcription factors, transporters, germination, sporulation, and flagellar assembly. However, in $Vdr^{-/-}$ mice, from the cecal to fecal microbiome (**Figure 6B**), we found an enrichment of modules related to the synthesis and degradation of metabolites or to diseases, such as pertussis, prostate cancer, and type I diabetes mellitus, as well as modules related to the biosynthesis of vancomycin-group antibiotics and streptomycin, whereas modules for transporters, cell cycle of *Caulobacter,* sporulation, prion diseases, and detoxification were reduced. Some modules were affected in both $Vdr^{-/-}$ and WT mice; for example, we detected increases in lipopolysaccharide biosynthesis, glycan biosynthesis and metabolism, and protein digestion and absorption, as well as decreases in sporulation and electron transfer, suggesting that these events are less likely related to the genetic difference. Consistent with what we found on comparing the $Vdr^{-/-}$ and WT samples, the fact that in the transition from the cecal to fecal microbiome detoxification by microbiota was weakened in $Vdr^{-/-}$ mice suggests that the colon is the major segment of the intestine subjected to the negative influences of unbalanced microbiota.

DISCUSSION

The findings from our study suggest that VDR status influences the intestinal microbiome at both the taxonomic and functional levels and correlates the VDR-associated bacterial changes in clinical diseases. Differences in the microbiomes of the different segments of the intestine were also evaluated. We report that VDR is crucial for the maintenance and "fine-tuning" of host–microbe interactions and therefore plays a key role in intestinal and microbial homeostasis.

On the taxonomic level, the Lactobacillales-to-*Lactobacillus* lineage was decreased in $Vdr^{-/-}$ fecal stool samples, correlating VDR with bacteria that produce lactic acid, which benefits the intestine by

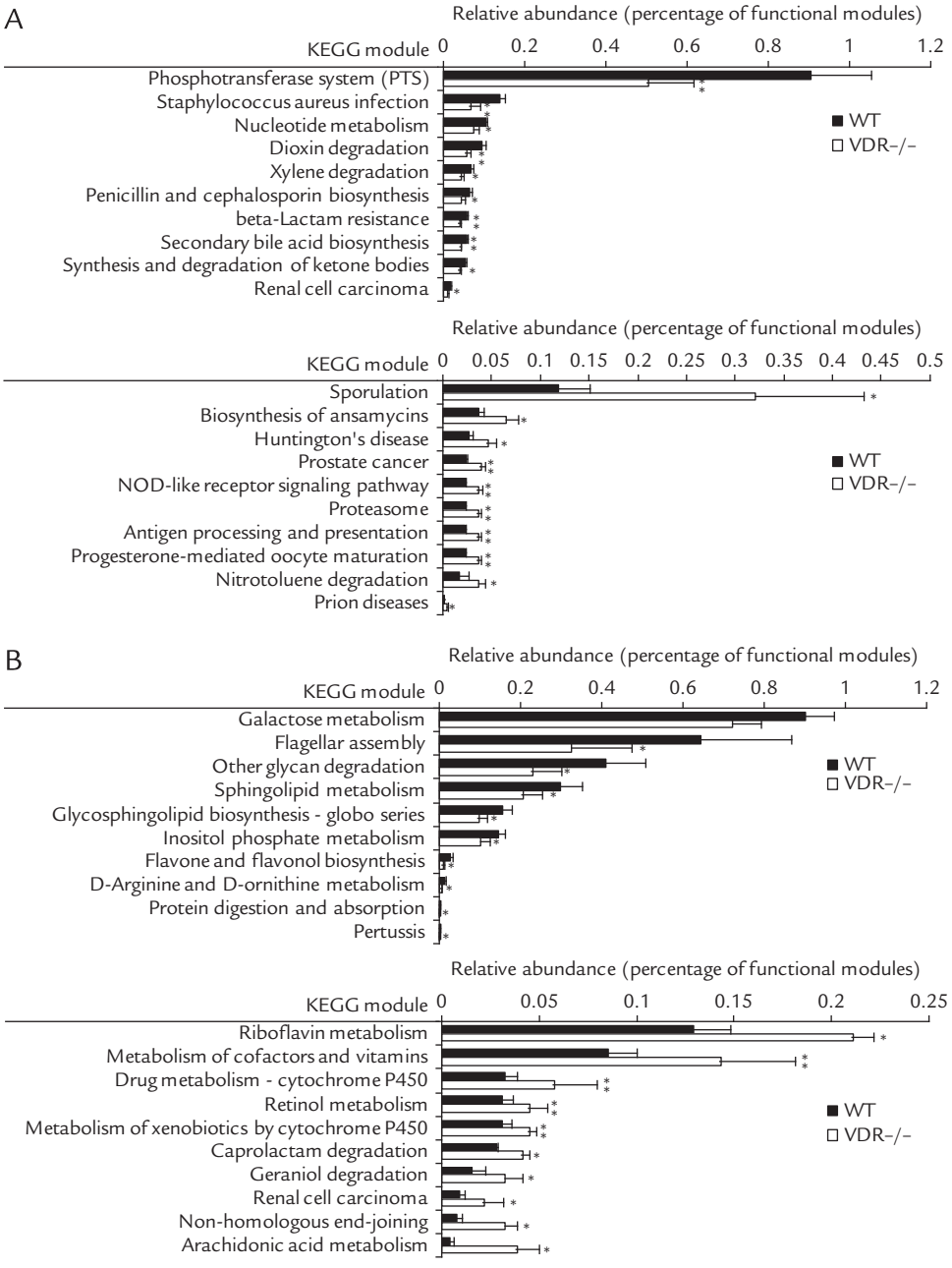

Figure 5. Functional alterations of the intestinal microbiome related to vitamin D receptor (VDR) status. Top 10 enriched and top 10 depleted Kyoto Encyclopedia of Genes and Genomes (KEGG) modules in the microbiome of fecal (A) and cecal (B) samples from $Vdr^{-/-}$ mice (n = 5) and WT mice (n = 3). Phylotypic Investigation of Communities by Reconstruction of Unobserved States (PICRUSt), version 1.0.0, in combination with HMP Unified Metabolic Analysis Network (HUMAnN), version 0.99,[22] would be used for comparing the abundances of bacterial gene modules by reference to the KEGG and Clusters of Orthologous Groups (COG) databases. KEGG modules related to amino acid, carbohydrate, and fatty acid synthesis and metabolism, detoxification, several signal pathways, infections, cancer, and other diseases were affected by Vdr status. $^{*}P < 0.05$; $^{**}P < 0.01$; $^{***}P < 0.001$.

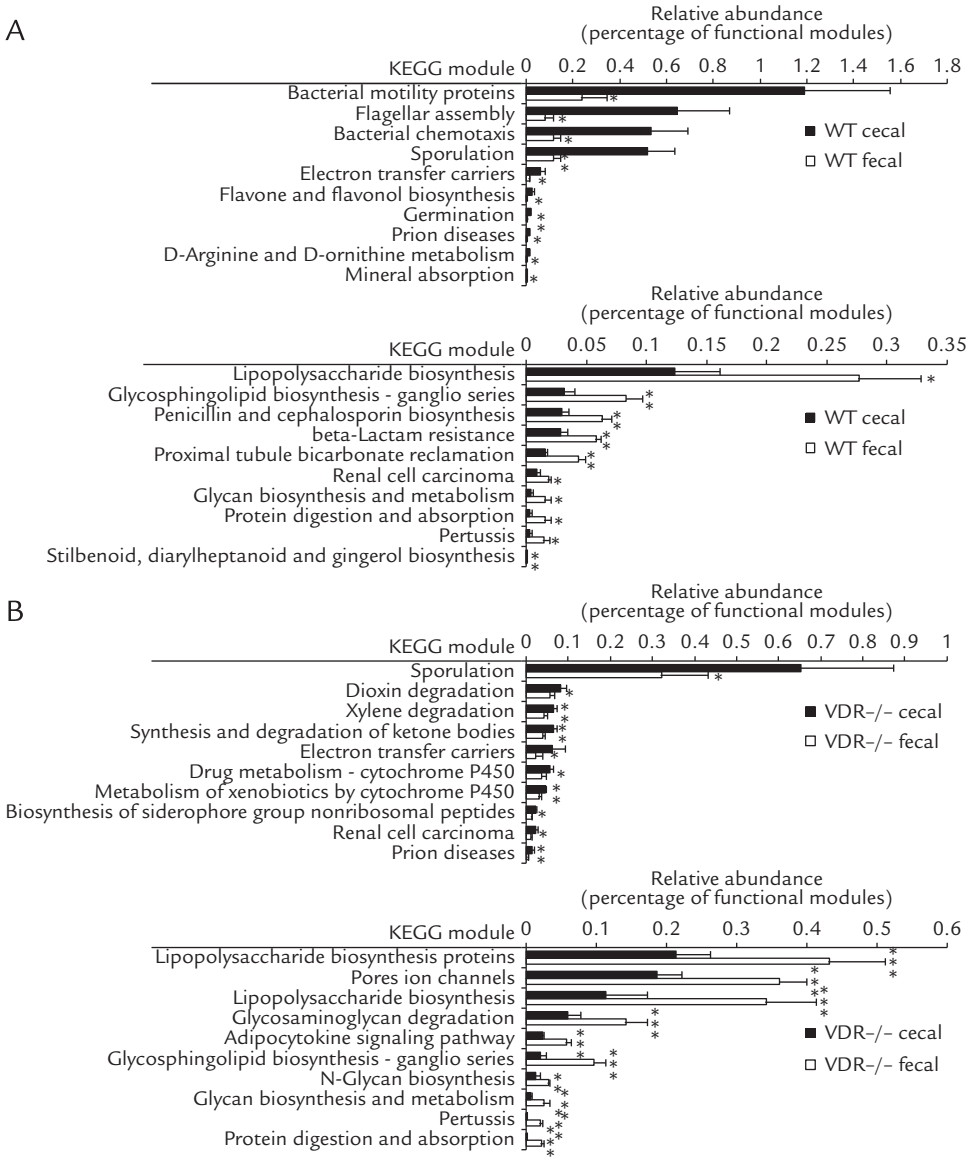

Figure 6. Functional alterations in intestinal microbiomes of different intestinal origins. Top 10 enriched and top 10 depleted Kyoto Encyclopedia of Genes and Genomes (KEGG) modules in the microbiomes of fecal stool compared with that of cecal contents from WT mice (A; n = 3) and $Vdr^{-/-}$ mice (B; n = 5). Phylotypic Investigation of Communities by Reconstruction of Unobserved States (PICRUSt), version 1.0.0, in combination with HMP Unified Metabolic Analysis Network (HUMAnN), version 0.99,[22] would be used for comparing the abundances of bacterial gene modules by reference to KEGG and Clusters of Orthologous Groups (COG) databases. In the transition from cecal to fecal microbiome, some KEGG modules were similarly affected in $Vdr^{-/-}$ and WT mice, such as enriched lipopolysaccharide biosynthesis, glycan biosynthesis and metabolism, protein digestion and absorption, and depleted sporulation, electron transfers. In the $Vdr^{-/-}$ mice, the transition is accompanied by a weakened capacity of detoxification and enriched antibiotic-producing modules like biosynthesis of vancomycin group antibiotics and streptomycin. $^{*}P < 0.05$; $^{**}P < 0.01$; $^{***}P < 0.001$.

lowering the pH and balancing the microflora[26] and also by its anti-inflammatory[27–29] and antitumor features.[30–32] In $Vdr^{-/-}$ fecal stool, the increased levels of *Bacteroides* may predispose the mice to colon cancer,[33] consistent with the observation that $Vdr^{-/-}$ mice are more prone to colonic tumorigenesis. Quite a number of species of *Clostridium* can be pathogenic and have been correlated with colitis, enteritis, and food poisoning.[34–37] The fact that *Clostridium* was enriched in $Vdr^{-/-}$ fecal stool therefore potentially increased the risks for gut disorders. *Alistipes, Odoribacter,* and *Eggerthella* were altered in the cecal stool of $Vdr^{-/-}$ mice. However, the cecum may not be the site where Vdr exerts its primary effects, because the microbial profile of cecal samples was not changed as dramatically as it was in fecal samples. Specifically, *Eggerthella* were enriched in cecal stool of $Vdr^{-/-}$ mice, which may be correlated with abdominal sepsis, IBD, and bacteremia.[38,39] This increase may pose a devastating threat to intestinal health. In the present study, its enrichment was restricted only in the cecum. In comparison to those in fecal microbiota, the genera affected by *Vdr* status in cecal microbiota were much less in relative abundance in both WT and $Vdr^{-/-}$ mice, implying that colon may be the major site of microbiome regulation.

Functionally, gut microbiota fulfill a series of important roles, including: (1) digestion of food ingredients to glean extra energy and synthesis of bioactive factors; (2) detoxification; (3) stimulation of epithelial healing and homeostasis; (4) exclusion of pathogens by competing for nutrients and binding sites and by antimicrobial secretions; (5) stimulation of the maturation of both innate and adaptive immunity; and (6) behavioral patterns and cardiac size.[1,40] In this study, the microbiome was categorized into functional modules by PICRUSt analysis.[22–24] We found that the functional relevance of Vdr status mainly manifested in nutrient metabolism and synthesis, indicating a crucial role for VDR in regulating the nutritional pattern determined by the microbiome. DNA repair, cell cycle, motility, and transporters accounted for a minor part of the affected functional modules. Overall, the data suggest that the $Vdr^{-/-}$ mice had higher risks for infections, cancer, inflammation, and other conditions.

In the present study, littermates were selected by genotyping and were cohoused before the experiments were performed; therefore, the influences of external factors could be mostly ruled out, and differences in the microbiomes of the $Vdr^{-/-}$ and WT mice could be ascribed to the genotypes. A number of genes were enriched or depleted in the microbiome of $Vdr^{-/-}$ mice (eg, dioxin degradation, prostate cancer in fecal samples, Nlr signaling), which provide a combination of microbial markers for diagnosing VDR deficiency. The switch from the cecal to the fecal environment is accompanied by dramatic enrichment of modules for metabolism and biosynthesis; increased risks for pertussis, diabetes mellitus, tuberculosis, and renal cell carcinoma and other cancer pathways; as well as reduced bacterial growth, motility, transporters, sporulation, germination, and detoxification. In the colon, the microbiome may therefore play an important role in the digestion and generation of metabolites for the host where bacterial growth and migration may not be as necessary or where these functions are inhibited by the host. In WT mice, detoxification modules were not affected in fecal compared with cecal contents, but they were reduced in $Vdr^{-/-}$ mice, suggesting physiologic disadvantages of the mutations. In the $Vdr^{-/-}$ mice, the biosynthesis of vancomycin-group antibiotics and streptomycin was increased; this change could dramatically alter the bacterial pattern, disturbing bacterial homeostasis.

VDR polymorphisms have been correlated with type II diabetes mellitus, and *VDR* mutations have been shown to contribute to its pathogenesis.[41] We consistently detected an increase in the KEGG module for type II diabetes mellitus in the cecal microbiome of *Vdr* knockout mice. Some polymorphisms in *VDR* have been associated with renal cell carcinoma in specific populations, but the correlation remains to be confirmed.[42–44] Variations in *VDR* may also affect the risk for prostate cancer.[45] In general, VDR is antiproliferative and has a protective role against malignancy. In this study, we detected an increase in the KEGG module of microbiota related to prostate cancer in fecal samples as well as an increase in the module related to renal cell carcinoma in cecal samples, indicating that the antitumor effects of VDR may also be executed through the intestinal microbiome. Vitamin D/VDR signaling is crucial for immunomodulation and immune responses,[46,47] especially in intestinal mucosa.[48] Our findings support this notion. For example, *Vdr* knockout led to an

increase in KEGG modules of microbiota related to antigen processing and presentation in fecal samples and a decrease in those related to pertussis in cecal samples.

Causes of IBD have been ascribed to a comprehensive list of factors, including genes, environment, immune responses, and microbiota.[49] In this study, KEGG modules related to peroxisome proliferator-activated receptor ($P < 0.01$), Nlr ($P < 0.01$), and mitogen-activated protein kinase ($P < 0.01$) signaling pathways were significantly upregulated in the fecal microbiome of $Vdr^{-/-}$ mice compared with that in WT mice (see **Supplemental Tables I–IV** in the online version at http://dx.doi.org/10.1016/j.clinthera.2015.04.004). Although all of them are closely related to immunity and inflammatory statuses, the enriched KEGG module related to Nlr signaling appeared to be of particular importance, because *NOD2* is among the 3 most often-defined genes underlying the risk for IBD.[5] Still unknown is how much other NLRs were affected and to what extent the altered NLR signaling–related KEGG module manifests the disturbance of the normal NLR signaling and cellular outcome in the hosts. But it did provide a strong indication that *Vdr* knockout might lead to abnormal Nod2 signaling and other aspects of Nlr signaling and increase murine susceptibility to dextran sodium sulfate–induced colitis and intestinal inflammation, as previously observed.[50,51] Studies have reported a correlation between transmissible bacteria and susceptibility to IBD, such as by fecal microbiota transplantation (FMT) in Nod2 mice and cohousing of Atg16l mice.[15,50] In addition to upregulation of CAMPs and extermination of *Mycobacterium tuberculosis* in monocytes,[16] intestinal epithelial VDR regulates autophagy and Paneth cells through the autophagy gene *ATG16L1,* thus changing the microbiome profile.[15] VDR controls gene expression in cooperation with certain transcriptional factors.[13–15,52] Overall, VDR mediates gene expression, inflammation, and the microbiota of the intestinal tract, therefore playing a crucial role in intestinal homeostasis.

We recognize that the limited number of mice available prevented us from further mining information from the data. The full *Vdr* knockout is pleiotropic, with symptoms such as growth retardation, flat face, compensatory parathyroid hyperplasia, and alopecia.[53] The design of future studies should include more samples and possibly introduce intestinal epithelial conditional *Vdr* knockout mice, which have been used by our laboratory. Because the PICRUSt analysis revealed that Vdr status influenced KEGG modules related to metabolism, future experiments in the metabolome may obtain additional findings. In addition, bioinformatic predictions of physiologic relevance cannot substitute for biochemical and histologic tests, which were not performed in the present study. Therefore, the Vdr-associated functions of the intestinal microbiota found in the present study will require verification by molecular assays. In the future, we can attempt to restore Vdr-associated dysbiotic changes by FMT, the full-spectrum transfer of microbiota from one host to another, or, vice versa, to transfer Vdr deficiency-associated phenotypes by FMT from a defective host.

Based on a literature search, the present study is the first attempt to decipher the influences of Vdr on functions of the intestinal microbiome. We also compared the microbiomes of different segments of the intestinal tract. Our study fills knowledge gaps by having investigated Vdr regulation of the intestinal microbial profile. The illustration of the microbial profiles of the mouse gut improves our understanding of the physiologic role of VDR and how VDR exerts its effects, therefore casting light on clinical therapeutics[54] that restore VDR function and healthy microbe–host interactions.

CONCLUSIONS

The present study fills knowledge gaps by having investigated the microbial profile affected by Vdr. Insights from our findings can be exploited to develop novel strategies to treat or prevent various diseases by restoring VDR function and healthy microbe–host interactions.

ACKNOWLEDGMENTS

This work was supported by the Swim Across America Cancer Research Award and Piccolo/Gavers Cancer Award to Jun Sun. We sincerely thank David Gerard, Rush University, for revising and proofreading the manuscript. The study sponsors were not involved in the collection, analysis, and interpretation of data; in the writing of the manuscript; or in the decision to submit the manuscript for publication.

CONFLICTS OF INTEREST

The authors have indicated that they have no conflicts of interest with regard to the content of this article.

SUPPLEMENTAL MATERIAL

Supplemental tables accompanying this article can be found in the online version at http://dx.doi.org/10.1016/j.clinthera.2015.04.004.

REFERENCES

1. Turnbaugh PJ, Ley RE, Hamady M, et al. The Human Microbiome Project. *Nature*. 2007;449:804–810.
2. Evans JM, Morris LS, Marchesi JR. The gut microbiome: The role of a virtual organ in the endocrinology of the host. *J Endocrinol*. 2013;218:R37–R47.
3. Ley RE, Lozupone CA, Hamady M, et al. Worlds within worlds: Evolution of the vertebrate gut microbiota. *Nat Rev Microbiol*. 2008;6:776–788.
4. Gurwitz D. The gut microbiome: Insights for personalized medicine. *Drug Dev Res*. 2013;74:341–343.
5. Jin D, Zhang H, Sun J. Manipulation of microbiome, a promising therapy for inflammatory bowel diseases. *J Clin Cell Immunol*. 2014;5:234.
6. Scaldaferri F, Gerardi V, Lopetuso LR, et al. Gut microbial flora, prebiotics, and probiotics in IBD: their current usage and utility. *Biomed Res Int*. 2013;2013:435268.
7. Manichanh C, Borruel N, Casellas F, Guarner F. The gut microbiota in IBD. *Nat Rev Gastroenterol Hepatol*. 2012;9:599–608.
8. Zak-Golab A, Olszanecka-Glinianowicz M, Kocelak P, Chudek J. The role of gut microbiota in the pathogenesis of obesity. *Postepy Hig Med Dosw (Online)*. 2014;68:84–90.
9. Hsiao EY, McBride SW, Hsien S, et al. Microbiota modulate behavioral and physiological abnormalities associated with neurodevelopmental disorders. *Cell*. 2013;155:1451–1463.
10. Bhattacharjee S, Lukiw WJ. Alzheimer's disease and the microbiome. *Front Cell Neurosci*. 2013;7:153.
11. Kim JH, Yamaori S, Tanabe T, et al. Implication of intestinal VDR deficiency in inflammatory bowel disease. *Biochim Biophys Acta*. 2013;1830:2118–2128.
12. Reich KM, Fedorak RN, Madsen K, Kroeker KI. Vitamin D improves inflammatory bowel disease outcomes: Basic science and clinical review. *World J Gastroenterol*. 2014;20:4934–4947.
13. Gombart AF. The vitamin D-antimicrobial peptide pathway and its role in protection against infection. *Future Microbiol*. 2009;4:1151–1165.
14. Campbell Y, Fantacone ML, Gombart AF. Regulation of antimicrobial peptide gene expression by nutrients and by-products of microbial metabolism. *Eur J Nutr*. 2012;51:899–907.
15. Wu S, Zhang Y-G, Lu R, et al. Intestinal epithelial vitamin D receptor deletion leads to defective autophagy in colitis. *Gut*. 2014;30. [Epub ahead of print].
16. Liu PT, Stenger S, Tang DH, Modlin RL. Cutting edge: vitamin D-mediated human antimicrobial activity against *Mycobacterium tuberculosis* is dependent on the induction of cathelicidin. *J Immunol*. 2007;179:2060–2063.
17. Ooi JH, Li Y, Rogers CJ, Cantorna MT. Vitamin D regulates the gut microbiome and protects mice from dextran sodium sulfate-induced colitis. *J Nutr*. 2013;143:1679–1686.
18. Li YC, Pirro AE, Amling M, et al. Targeted ablation of the vitamin D receptor: An animal model of vitamin D-dependent rickets type II with alopecia. *Proc Natl Acad Sci U S A*. 1997;94:9831–9835.
19. Edgar RC. Search and clustering orders of magnitude faster than BLAST. *Bioinformatics*. 2010;26:2460–2461.
20. Edgar RC, Haas BJ, Clemente JC, et al. UCHIME improves sensitivity and speed of chimera detection. *Bioinformatics*. 2011;27:2194–2200.
21. Caporaso JG, Kuczynski J, Stombaugh J, et al. QIIME allows analysis of high-throughput community sequencing data. *Nat Methods*. 2010;7:335–336.
22. Abubucker S, Segata N, Goll J, et al. Metabolic reconstruction for metagenomic data and its application to the human microbiome. *PLoS Comput Biol*. 2012;8:e1002358.
23. Kanehisa M, Goto S, Sato Y, et al. KEGG for integration and interpretation of large-scale molecular data sets. *Nucleic Acids Res*. 2012;40:D109–D114.
24. Tatusov RL, Koonin EV, Lipman DJ. A genomic perspective on protein families. *Science*. 1997;278:631–637.
25. McHardy IH, Li X, Tong M, et al. HIV Infection is associated with compositional and functional shifts in the rectal mucosal microbiota. *Microbiome*. 2013;1:26.
26. Salminen S, Salminen E. Lactulose, lactic acid bacteria, intestinal microecology and mucosal protection. *Scand J Gastroenterol Suppl*. 1997;222:45–48.
27. Maekawa T, Hajishengallis G. Topical treatment with probiotic *Lactobacillus brevis* CD2 inhibits experimental periodontal inflammation and bone loss. *J Periodontal Res*. 2014;49:785–791.
28. Park JE, Oh SH, Cha YS. *Lactobacillus brevis* OPK-3 isolated from kimchi inhibits adipogenesis and exert anti-inflammation in 3T3-L1 adipocyte. *J Sci Food Agric*. 2014;94:2514–2520.
29. Thiraworawong T, Spinler JK, Werawatganon D, et al. Anti-inflammatory properties of gastric-derived *Lactobacillus plantarum* XB7 in the context of *Helicobacter pylori* infection. *Helicobacter*. 2014;19:144–155.
30. Fukui M, Fujino T, Tsutsui K, et al. The tumor-preventing effect of a mixture of several lactic acid bacteria on 1,2-dimethylhydrazine-induced colon carcinogenesis in mice. *Oncol Rep*. 2001;8:1073–1078.

31. Kandasamy M, Bay BH, Lee YK, Mahendran R. Lactobacilli secreting a tumor antigen and IL15 activates neutrophils and dendritic cells and generates cytotoxic T lymphocytes against cancer cells. *Cell Immunol*. 2011;271:89–96.
32. Han DJ, Kim JB, Park SY, et al. Growth inhibition of hepatocellular carcinoma Huh7 cells by *Lactobacillus casei* extract. *Yonsei Med J*. 2013;54:1186–1193.
33. Zackular JP, Baxter NT, Iverson KD, et al. The gut microbiome modulates colon tumorigenesis. *MBio*. 2013;4:e00692–00613.
34. Antharam VC, Li EC, Ishmael A, et al. Intestinal dysbiosis and depletion of butyrogenic bacteria in *Clostridium difficile* infection and nosocomial diarrhea. *J Clin Microbiol*. 2013;51:2884–2892.
35. Chen J, Ma M, Uzal FA, McClane BA. Host cell-induced signaling causes *Clostridium perfringens* to upregulate production of toxins important for intestinal infections. *Gut Microbes*. 2013;5:96–107.
36. Gould LH, Walsh KA, Vieira AR, et al. Surveillance for foodborne disease outbreaks—United States, 1998-2008. *MMWR Surveill Summ*. 2013;62:1–34.
37. Fitzpatrick LR, Small JS, Greene WH, et al. *Bacillus coagulans* GBI-30, 6086 limits the recurrence of *Clostridium difficile*-induced colitis following vancomycin withdrawal in mice. *Gut Pathog*. 2012; 4:13.
38. Gardiner BJ, Korman TM, Junckerstorff RK. Eggerthella lenta bacteraemia complicated by spondylodiscitis, psoas abscess and meningitis. *J Clin Microbiol*. 2014;52:1278–1280.
39. Thota VR, Dacha S, Natarajan A, Nerad J. *Eggerthella lenta* bacteremia in a Crohn's disease patient after ileocecal resection. *Future Microbiol*. 2011;6:595–597.
40. O'Hara AM, Shanahan F. The gut flora as a forgotten organ. *EMBO Rep*. 2006;7:688–693.
41. Manchanda PK, Bid HK. Vitamin D receptor and type 2 diabetes mellitus: Growing therapeutic opportunities. *Indian J Hum Genet*. 2012;18:274–275.
42. Gandini S, Gnagnarella P, Serrano D, et al. Vitamin D receptor polymorphisms and cancer. *Adv Exp Med Biol*. 2014;810:69–105.
43. Khan MI, Bielecka ZF, Najm MZ, et al. Vitamin D receptor gene polymorphisms in breast and renal cancer: Current state and future approaches. *Int J Oncol*. 2014;44: 349–363.
44. Ou C, Zhao HL, Zhu B, et al. Association of vitamin D receptor gene polymorphism with the risk of renal cell carcinoma: A meta-analysis. *J Recept Signal Transduct Res*. 2014;34:463–468.
45. Zhang Q, Shan Y. Genetic polymorphisms of vitamin D receptor and the risk of prostate cancer: a meta-analysis. *J BUON*. 2013;18:961–969.
46. Adorini L, Penna G. Control of autoimmune diseases by the vitamin D endocrine system. *Nat Clin Pract Rheumatol*. 2008;4:404–412.
47. Blaney GP, Albert PJ, Proal AD. Vitamin D metabolites as clinical markers in autoimmune and chronic disease. *Ann N Y Acad Sci*. 2009;1173:384–390.
48. Sun J. Vitamin D and mucosal immune function. *Curr Opin Gastroenterol*. 2010;26:591–595.
49. Sartor RB. Key questions to guide a better understanding of host-commensal microbiota interactions in intestinal inflammation. *Mucosal Immunol*. 2011;4:127–132.
50. Couturier-Maillard A, Secher T, Rehman A, et al. NOD2-mediated dysbiosis predisposes mice to transmissible colitis and colorectal cancer. *J Clin Invest*. 2013;123:700–711.
51. Kong J, Zhang Z, Musch MW, et al. Novel role of the vitamin D receptor in maintaining the integrity of the intestinal mucosal barrier. *Am J Physiol Gastrointest Liver Physiol*. 2008;294:G208–G216.
52. Goeman F, De Nicola F, D'Onorio De Meo P, et al. VDR primary targets by genome-wide transcriptional profiling. *J Steroid Biochem Mol Biol*. 2014;143:348–356.
53. Hofbauer LC, Heufelder AE. Vitamin D receptor knock-out mice: the expectational and the exceptional. *Eur J Endocrinol*. 1998;138:372–373.
54. Sun J, Chang EB. Exploring gut microbes in human health and disease: pushing the envelope. *Genes Dis*. 2014;1:132–139.

Address for correspondence: Jun Sun, PhD, Department of Biochemistry, Rush University Medical Center, 1735 West Harrison Street, Chicago, IL 60612. E-mail: jun_sun@rush.edu

SUPPLEMENTARY MATERIAL

Supplemental Table I. Total abundance of functional modules in the fecal microbiomes of vitamin D receptor gene knockout ($Vdr^{-/-}$) and wild-type (WT) mice.

Substance	$Vdr^{-/-}$ Fecal		WT Fecal		Fold Change, $Vdr^{-/-}$ to WT	*P*
	Mean	SD	Mean	SD		
Prion diseases	4.64E-05	1.79E-05	1.41E-05	1.11E-05	3.298085	0.032329
Sporulation	0.003211	0.001126	0.001193	0.000331	2.691036	0.025904
Nitrotoluene degradation	0.00037	7.32E-05	0.000174	0.000103	2.123957	0.019068
Biosynthesis of ansamycins	0.000656	0.000122	0.000372	6.12E-05	1.764205	0.010337
Huntington disease	0.000465	9.96E-05	0.000266	5.66E-05	1.744314	0.021215
Prostate cancer	0.000391	5.78E-05	0.000236	2.35E-05	1.659676	0.004912
NOD-like receptor signaling pathway	0.000364	4.75E-05	0.000229	2.02E-05	1.587158	0.003886
Proteasome	0.000362	4.73E-05	0.000229	2.04E-05	1.582677	0.003994
Antigen processing and presentation	0.000362	4.73E-05	0.000229	2.04E-05	1.582677	0.003994
Progesterone-mediated oocyte maturation	0.000362	4.73E-05	0.000229	2.04E-05	1.582677	0.003994
Epithelial cell signaling in *Helicobacter pylori* infection	0.000727	0.000132	0.00046	3.5E-05	1.579354	0.01592
Isoquinoline alkaloid biosynthesis	0.000447	4.65E-05	0.00029	5.4E-05	1.538893	0.004769
Porphyrin and chlorophyll metabolism	0.004607	0.000961	0.003015	0.000465	1.527891	0.039119
Biosynthesis and biodegradation of secondary metabolites	0.000551	4.71E-05	0.000369	0.000104	1.494327	0.012824
Adipocytokine signaling pathway	0.000569	8.91E-05	0.000389	6.67E-05	1.462434	0.024324
Ascorbate and aldarate metabolism	0.000858	0.000102	0.00059	0.00011	1.454582	0.012552
Phenylalanine, tyrosine and tryptophan biosynthesis	0.006639	0.000733	0.004645	0.000353	1.429314	0.004995
Lysine degradation	0.001268	0.000196	0.0009	0.000224	1.409494	0.049571
MAPK signaling pathway—yeast	0.000509	5.65E-05	0.000363	6.06E-05	1.401181	0.013701
Phenylpropanoid biosynthesis	0.001452	0.000187	0.001039	0.000153	1.398277	0.018295
Cell division	0.00068	8.96E-05	0.000492	0.000115	1.383082	0.04021
Phenylalanine metabolism	0.001637	0.000111	0.001198	0.00028	1.366679	0.017524
Tropane, piperidine and pyridine alkaloid biosynthesis	0.000982	5.87E-05	0.000719	8.49E-05	1.366434	0.001895
Novobiocin biosynthesis	0.001155	9.8E-05	0.000854	6.8E-05	1.352515	0.003598
C5-branched dibasic acid metabolism	0.002502	0.000241	0.001891	0.000187	1.323346	0.00976
Histidine metabolism	0.006148	0.000307	0.004823	0.000355	1.27458	0.001384
Pentose and glucuronate interconversions	0.004337	0.00036	0.003422	0.000124	1.267635	0.006067
Peroxisome	0.001797	0.000203	0.001434	0.000192	1.253159	0.04718
Glyoxylate and dicarboxylate metabolism	0.004485	0.000276	0.003638	0.000344	1.232728	0.008344
Energy metabolism	0.009168	0.000565	0.00745	0.000566	1.230619	0.005936
beta-Alanine metabolism	0.001947	0.000148	0.001586	0.000161	1.227986	0.017526
PPAR signaling pathway	0.000934	4.91E-05	0.000783	5.69E-05	1.193565	0.007095
Arginine and proline metabolism	0.011298	0.000713	0.009478	0.000569	1.191978	0.009765
Carbohydrate metabolism	0.001179	3.84E-05	0.001	0.000164	1.179682	0.048682
Valine, leucine and isoleucine biosynthesis	0.006606	0.000364	0.005633	0.000585	1.172742	0.025224
Plant-pathogen interaction	0.001323	0.000106	0.001149	1.29E-05	1.150811	0.033663
Glycine, serine and threonine metabolism	0.00856	0.000104	0.007715	0.000339	1.109523	0.001631
Other transporters	0.002141	1.66E-05	0.001934	0.000131	1.106631	0.010291
Butirosin and neomycin biosynthesis	0.000848	1.04E-05	0.000792	3.08E-05	1.071173	0.007807
Pantothenate and CoA biosynthesis	0.00594	0.000228	0.005546	0.000185	1.070958	0.045905
Cysteine and methionine metabolism	0.008962	0.00013	0.008591	0.000237	1.043173	0.026401
Bacterial toxins	0.00141	3.77E-05	0.001493	3.47E-05	0.944695	0.02174
DNA repair and recombination proteins	0.030697	0.000932	0.032645	0.001217	0.940335	0.042048
Nucleotide excision repair	0.004284	9.14E-05	0.004559	7.56E-05	0.939731	0.004809
Peptidoglycan biosynthesis	0.008357	0.000236	0.008931	0.000375	0.935728	0.035113
Terpenoid backbone biosynthesis	0.00628	0.000202	0.006811	0.000292	0.921942	0.021528
Purine metabolism	0.024505	0.000939	0.026588	0.000617	0.921641	0.014941
Aminoacyl-tRNA biosynthesis	0.012922	0.000201	0.014084	0.000588	0.917474	0.005557
Glycerolipid metabolism	0.004269	0.000217	0.004695	8.33E-05	0.909354	0.019199
Photosynthesis proteins	0.003839	0.000192	0.004225	0.000242	0.908482	0.045433
Amino sugar and nucleotide sugar metabolism	0.016035	0.000803	0.017673	0.000377	0.907275	0.017498
Photosynthesis	0.00382	0.000195	0.004216	0.000241	0.906105	0.042677
Prenyltransferases	0.004057	0.00028	0.00464	0.000132	0.874253	0.01607

(continued)

Supplemental Table 1. (continued).

Substance	$Vdr^{-/-}$ Fecal		WT Fecal		Fold Change, $Vdr^{-/-}$ to WT	*P*
	Mean	SD	Mean	SD		
Galactose metabolism	0.007537	0.000298	0.00877	0.001026	0.859437	0.038715
Glycolysis/gluconeogenesis	0.012319	0.000775	0.014442	0.000397	0.853014	0.004982
Fructose and mannose metabolism	0.010457	0.001202	0.012302	0.000337	0.850013	0.045022
Signal transduction mechanisms	0.004534	0.000362	0.005343	0.000298	0.848592	0.017664
RNA transport	0.001478	0.000142	0.001752	8.76E-05	0.843922	0.025364
RNA polymerase	0.001917	0.000104	0.002283	0.000109	0.839359	0.003172
Glycosyltransferases	0.003987	0.000462	0.004782	0.000256	0.83365	0.036149
D-Alanine metabolism	0.001376	9.5E-05	0.001713	0.000136	0.803306	0.00584
Primary bile acid biosynthesis	0.000433	1.9E-05	0.000565	5.62E-05	0.765569	0.002361
Secondary bile acid biosynthesis	0.000432	2.08E-05	0.000564	5.46E-05	0.765012	0.002299
Synthesis and degradation of ketone bodies	0.000402	5.6E-05	0.000537	5.67E-05	0.74737	0.016282
Nucleotide metabolism	0.000756	0.000138	0.001038	4.87E-05	0.728427	0.015734
Penicillin and cephalosporin biosynthesis	0.000457	0.000102	0.00063	8.43E-05	0.725093	0.048993
β-Lactam resistance	0.000393	7.61E-05	0.000581	4.28E-05	0.676055	0.008431
Xylene degradation	0.00043	9.4E-05	0.000671	9.24E-05	0.641212	0.01239
Renal cell carcinoma	0.000113	3.69E-05	0.000183	2.53E-05	0.615278	0.027984
Dioxin degradation	0.000568	0.000128	0.000956	0.000125	0.593928	0.005824
Phosphotransferase system (PTS)	0.005045	0.001154	0.009064	0.001503	0.556639	0.005115
Staphylococcus aureus infection	0.000677	0.000242	0.001395	0.000136	0.485215	0.003574

Supplemental Table II. Total abundance of functional modules in the cecal microbiomes of vitamin D receptor gene knockout ($Vdr^{-/-}$) and wild-type (WT) mice.

Substance	$Vdr^{-/-}$ Cecal		WT Cecal		Fold Change, $Vdr^{-/-}$ to WT	*P*
	Mean	SD	Mean	SD		
Arachidonic acid metabolism	0.000386	0.000207	4.55E-05	2.33E-05	8.475838	0.033481
Nonhomologous end-joining	0.000327	0.000116	7.76E-05	2.83E-05	4.213825	0.011795
Renal cell carcinoma	0.000218	6.57E-05	8.85E-05	3.57E-05	2.464992	0.021432
Geraniol degradation	0.000328	0.000101	0.000158	7.16E-05	2.081122	0.044191
Drug metabolism—cytochrome P-450	0.000576	9.49E-05	0.000327	6.2E-05	1.763651	0.007134
Metabolism of cofactors and vitamins	0.001431	0.000226	0.000852	0.000155	1.680562	0.008318
Riboflavin metabolism	0.002112	0.00039	0.00129	0.000195	1.637011	0.015759
Caprolactam degradation	0.000415	8.88E-05	0.000282	1.29E-05	1.473584	0.04605
Metabolism of xenobiotics by cytochrome P-450	0.00045	3.97E-05	0.000313	5.17E-05	1.441043	0.005189
Retinol metabolism	0.00045	3.95E-05	0.000314	5.36E-05	1.435395	0.005776
Synthesis and degradation of ketone bodies	0.000651	0.000112	0.000468	6.63E-05	1.391024	0.044793
Sulfur relay system	0.002594	0.00025	0.001902	0.000167	1.363691	0.005721
Citrate cycle (TCA cycle)	0.0054	0.000703	0.004089	0.000676	1.320517	0.041503
Protein processing in endoplasmic reticulum	0.000669	8.18E-05	0.00052	7.3E-05	1.287437	0.041168
Glutathione metabolism	0.002524	0.000261	0.001963	0.00013	1.285371	0.014565
Type II diabetes mellitus	0.000523	6.8E-05	0.000414	2.39E-05	1.263106	0.040196
Fatty acid metabolism	0.002384	0.000275	0.001926	1.47E-05	1.238152	0.031543
Taurine and hypotaurine metabolism	0.001773	0.000144	0.001459	0.000176	1.215261	0.032708
Tuberculosis	0.001572	0.000102	0.001355	0.000125	1.159817	0.035961
Base excision repair	0.005249	0.000326	0.004529	0.000222	1.158877	0.015733
Glycerophospholipid metabolism	0.005974	0.000187	0.00523	0.000344	1.142262	0.006622
Propanoate metabolism	0.005791	0.000308	0.005153	0.000437	1.123875	0.049493
Other transporters	0.002219	0.000118	0.001998	0.000105	1.110128	0.037766
Bacterial toxins	0.001565	7.16E-05	0.001418	5.86E-05	1.104162	0.024189
Cysteine and methionine metabolism	0.008632	0.000432	0.007863	0.000305	1.097698	0.037125
Translation proteins	0.009297	0.000437	0.008503	0.000457	1.093379	0.049695
Selenocompound metabolism	0.00371	6.39E-05	0.003525	0.00012	1.052531	0.026442
General function prediction only	0.034715	0.000893	0.033172	0.000113	1.046495	0.027864
Methane metabolism	0.011181	0.00048	0.012449	0.000107	0.898122	0.004687
C5-branched dibasic acid metabolism	0.002037	0.000182	0.002407	0.000248	0.846406	0.049791
Galactose metabolism	0.007235	0.000714	0.009011	0.000727	0.802937	0.014762
Inositol phosphate metabolism	0.001032	0.000245	0.001445	0.0002	0.713903	0.049772
Sphingolipid metabolism	0.002064	0.000509	0.002998	0.000542	0.688428	0.04923
Glycosphingolipid biosynthesis—globo series	0.000968	0.00025	0.001559	0.000252	0.620956	0.017973
Other glycan degradation	0.002301	0.000749	0.004111	0.000984	0.559687	0.024993
Flagellar assembly	0.003258	0.001495	0.006459	0.002247	0.504462	0.049054
Flavone and flavonol biosynthesis	9.94E-05	6.87E-05	0.000257	9.93E-05	0.387333	0.036284
D-Arginine and D-ornithine metabolism	5.15E-05	3.68E-05	0.000134	4.73E-05	0.384669	0.032042
Pertussis	7.81E-06	8.19E-06	3.23E-05	2.07E-05	0.241557	0.049958
Protein digestion and absorption	7.56E-06	7.35E-06	3.32E-05	2.22E-05	0.227947	0.047912

Supplemental Table III. Total abundance of functional modules in the cecal and fecal microbiomes of wild-type (WT) mice.

Substance	WT Cecal		WT Fecal		Fold Change, Cecal to Fecal	*P*
	Mean	SD	Mean	SD		
Protein digestion and absorption	3.32E-05	2.22E-05	0.000153	5.97E-05	4.623081	0.030923
Stilbenoid, diarylheptanoid, and gingerol biosynthesis	1.44E-06	5.98E-07	6.53E-06	1.7E-06	4.5399	0.008023
Pertussis	3.23E-05	2.07E-05	0.000144	5.62E-05	4.444783	0.032379
Glycan biosynthesis and metabolism	4.32E-05	2.3E-05	0.000153	5.83E-05	3.549003	0.038225
Proximal tubule bicarbonate reclamation	0.000157	2.28E-05	0.000439	6.22E-05	2.792809	0.001812
Glycosphingolipid biosynthesis—ganglio series	0.000315	9.82E-05	0.000831	0.000142	2.636234	0.006656
Lipopolysaccharide biosynthesis	0.001233	0.000382	0.002768	0.000516	2.244594	0.014374
Penicillin and cephalosporin biosynthesis	0.000295	6.55E-05	0.00063	8.43E-05	2.131738	0.005596
Renal cell carcinoma	8.85E-05	3.57E-05	0.000183	2.53E-05	2.069985	0.019962
β-Lactam resistance	0.000289	5.84E-05	0.000581	4.28E-05	2.009693	0.002215
Glycosaminoglycan degradation	0.000663	0.000166	0.001236	0.000189	1.86521	0.016935
Restriction enzyme	0.000886	0.00032	0.001597	0.000211	1.801805	0.032694
Membrane and intracellular structural molecules	0.003204	0.000595	0.005659	0.00037	1.766255	0.00373
Toluene degradation	0.000753	0.000245	0.001273	5.43E-05	1.690323	0.022883
Ubiquinone and other terpenoid-quinone biosynthesis	0.001849	0.000281	0.003092	0.000155	1.67193	0.002579
Pores ion channels	0.001854	0.000286	0.003088	0.00028	1.66549	0.005937
Riboflavin metabolism	0.00129	0.000195	0.002138	0.000161	1.657526	0.004356
Biotin metabolism	0.000733	0.00014	0.001164	0.000122	1.58875	0.015754
Lipoic acid metabolism	0.000363	8.18E-05	0.000574	6.06E-05	1.579775	0.023161
Lipopolysaccharide biosynthesis proteins	0.00225	0.000396	0.003548	0.000483	1.576837	0.022803
Citrate cycle (TCA cycle)	0.004089	0.000676	0.0062	0.000507	1.51627	0.012395
Protein processing in endoplasmic reticulum	0.00052	7.3E-05	0.000781	4.16E-05	1.501552	0.005775
Prenyltransferases	0.003106	0.000546	0.00464	0.000132	1.49419	0.009091
β-Alanine metabolism	0.001138	0.000189	0.001586	0.000161	1.393889	0.035352
Folate biosynthesis	0.002647	0.00024	0.003656	0.000252	1.381205	0.007403
Type I diabetes mellitus	0.000494	6.09E-05	0.000673	8.35E-05	1.360995	0.040257
Secondary bile acid biosynthesis	0.000418	8.34E-06	0.000564	5.46E-05	1.350407	0.010118
Primary bile acid biosynthesis	0.000419	6.95E-06	0.000565	5.62E-05	1.348501	0.011133
Glycosyltransferases	0.003556	0.000313	0.004782	0.000256	1.344772	0.00632
Bacterial secretion system	0.004729	0.000455	0.006302	0.000706	1.332594	0.03156
D-Glutamine and D-glutamate metabolism	0.001433	0.000142	0.001885	0.000188	1.315452	0.029443
Alzheimer disease	0.00045	4.12E-05	0.000584	2.05E-05	1.29931	0.007166
Oxidative phosphorylation	0.008645	0.000567	0.011231	0.000487	1.299027	0.003911
Carbon fixation pathways in prokaryotes	0.007608	0.000828	0.009823	0.000469	1.291123	0.015744
Tuberculosis	0.001355	0.000125	0.001749	6.82E-05	1.290208	0.008658
Terpenoid backbone biosynthesis	0.005283	0.000631	0.006811	0.000292	1.289157	0.019039
Pathways in cancer	0.000323	2.6E-05	0.000412	7.95E-06	1.277314	0.004665
Type II diabetes mellitus	0.000414	2.39E-05	0.000527	2.96E-05	1.272101	0.00684
Taurine and hypotaurine metabolism	0.001459	0.000176	0.001847	7.61E-05	1.266212	0.024762
RNA degradation	0.004173	0.000377	0.005206	7.67E-05	1.247647	0.009641
Zeatin biosynthesis	0.000438	3.97E-05	0.000543	3.55E-05	1.23879	0.027196
Ribosome	0.023089	0.002132	0.028293	0.001925	1.225367	0.034916
Ribosome biogenesis in eukaryotes	0.000437	3.83E-05	0.000533	3.12E-05	1.218171	0.028699
Translation factors	0.00525	0.00036	0.00638	0.000372	1.215427	0.019405
Glutathione metabolism	0.001963	0.00013	0.002374	8.43E-05	1.209439	0.010123
Chaperones and folding catalysts	0.009256	0.000593	0.011187	0.000281	1.208683	0.006995
Glycerophospholipid metabolism	0.00523	0.000344	0.006281	0.000216	1.20111	0.010989
RNA polymerase	0.001916	0.000198	0.002283	0.000109	1.191935	0.047996
Replication, recombination and repair proteins	0.007488	0.000681	0.008925	0.000567	1.191904	0.04833
Biosynthesis of vancomycin group antibiotics	0.000605	1.63E-05	0.000717	2.98E-05	1.185069	0.00467
DNA replication	0.006549	0.000536	0.007737	0.000503	1.181306	0.048813
Nucleotide excision repair	0.003863	0.00022	0.004559	7.56E-05	1.18004	0.00663
Protein export	0.005589	0.000415	0.006581	0.000411	1.177633	0.042284
One carbon pool by folate	0.005537	0.000333	0.006509	0.000303	1.175548	0.020149
Ribosome Biogenesis	0.013368	0.00103	0.015621	0.000694	1.168549	0.03479
Mismatch repair	0.007849	0.000508	0.009145	0.000489	1.165198	0.033445
Pantothenate and CoA biosynthesis	0.00478	0.000236	0.005546	0.000185	1.160309	0.011441

(continued)

Supplemental Table III. (continued).

Substance	WT Cecal		WT Fecal		Fold Change, Cecal to Fecal	*P*
	Mean	SD	Mean	SD		
Photosynthesis	0.003636	0.000247	0.004216	0.000241	1.159442	0.043637
Base excision repair	0.004529	0.000222	0.005237	6.2E-05	1.156349	0.006018
DNA replication proteins	0.011692	0.000713	0.013496	0.000796	1.15431	0.043083
Cell cycle—*Caulobacter*	0.004967	0.000301	0.005726	0.000288	1.152891	0.034219
Glycolysis/gluconeogenesis	0.012608	0.000786	0.014442	0.000397	1.145467	0.022605
DNA repair and recombination proteins	0.028506	0.001652	0.032645	0.001217	1.145212	0.025026
Amino acid metabolism	0.001829	0.00012	0.002094	8.95E-05	1.145133	0.037147
Streptomycin biosynthesis	0.002955	0.000155	0.003355	0.000136	1.135442	0.028446
Purine metabolism	0.023494	0.001673	0.026588	0.000617	1.131711	0.039743
Thiamine metabolism	0.004264	0.000178	0.004818	0.00013	1.129979	0.012153
Translation proteins	0.008503	0.000457	0.009569	4.69E-05	1.125336	0.015894
Alanine, aspartate, and glutamate metabolism	0.009249	0.000266	0.010188	0.000469	1.101524	0.039356
Cysteine and methionine metabolism	0.007863	0.000305	0.008591	0.000237	1.092514	0.031005
Glutamatergic synapse	0.000898	3.69E-05	0.000976	2.47E-05	1.086844	0.038314
Amino acid related enzymes	0.014177	0.000398	0.015289	0.000405	1.078398	0.027525
General function prediction only	0.033172	0.000113	0.034391	0.000169	1.036746	0.000482
Pentose phosphate pathway	0.009019	0.000201	0.008438	0.000151	0.935566	0.016007
Glycerolipid metabolism	0.005502	0.000142	0.004695	8.33E-05	0.853282	0.001048
C5-branched dibasic acid metabolism	0.002407	0.000248	0.001891	0.000187	0.785438	0.045119
Plant–pathogen interaction	0.001479	8.15E-05	0.001149	1.29E-05	0.777037	0.002289
Transcription factors	0.020305	0.00126	0.014845	0.000512	0.731089	0.00225
ABC transporters	0.037074	0.003103	0.026059	0.001429	0.702872	0.005042
Two-component system	0.016029	0.002006	0.011005	0.001352	0.686539	0.022799
Pentose and glucuronate interconversions	0.005116	0.000825	0.003422	0.000124	0.668864	0.024513
Phosphonate and phosphinate metabolism	0.000737	0.000136	0.000482	7.1E-05	0.653983	0.044719
Transporters	0.091666	0.012021	0.058375	0.004447	0.636823	0.010833
Protein kinases	0.003532	0.000527	0.002199	0.000317	0.622698	0.019841
Carbohydrate metabolism	0.00168	0.000355	0.001	0.000164	0.595003	0.039283
Ascorbate and aldarate metabolism	0.001047	0.000232	0.00059	0.00011	0.56326	0.036521
Amyotrophic lateral sclerosis (ALS)	0.000327	7.16E-05	0.000164	4.98E-05	0.50119	0.031578
Biosynthesis of ansamycins	0.000788	0.000131	0.000372	6.12E-05	0.472084	0.007588
Porphyrin and chlorophyll metabolism	0.006854	0.001316	0.003015	0.000465	0.439878	0.008873
Germination	0.000193	3.61E-05	5.31E-05	5.23E-06	0.275619	0.002693
Electron transfer carriers	0.000601	0.000222	0.000141	1.64E-05	0.234743	0.023125
Sporulation	0.005211	0.001194	0.001193	0.000331	0.228982	0.004936
Bacterial chemotaxis	0.005356	0.001603	0.001182	0.000334	0.220732	0.011564
Mineral absorption	7.01E-06	2.24E-06	1.46E-06	1.72E-06	0.20777	0.027015
Bacterial motility proteins	0.011922	0.003677	0.002376	0.001123	0.199247	0.012639
Flagellar assembly	0.006459	0.002247	0.000796	0.000383	0.123287	0.012608
Flavone and flavonol biosynthesis	0.000257	9.93E-05	2.56E-05	1.77E-05	0.099901	0.016579
Prion diseases	0.000142	4.73E-05	1.41E-05	1.11E-05	0.099356	0.010417
D-Arginine and D-ornithine metabolism	0.000134	4.73E-05	1.19E-05	9.38E-06	0.088754	0.011845

Supplemental Table IV. Total abundance of functional modules in the cecal and fecal microbiomes of vitamin D receptor gene knockout ($Vdr^{-/-}$) mice.

Substance	$Vdr^{-/-}$ Cecal		$Vdr^{-/-}$ Fecal		Fold Change, Cecal To Fecal	*P*
	Mean	SD	Mean	SD		
Protein digestion and absorption	7.56E-06	7.35E-06	0.00021622	4.68406E-05	28.60644	9.57E-06
Pertussis	7.81E-06	8.19E-06	0.000195097	4.5237E-05	24.99046	1.69E-05
Glycosphingolipid biosynthesis—ganglio series	0.000199	9.84E-05	0.0009722	0.000173309	4.896001	2.41E-05
Glycan biosynthesis and metabolism	6.36E-05	3.01E-05	0.000253472	8.6275E-05	3.988096	0.001648
Lipopolysaccharide biosynthesis	0.001144	0.000588	0.003421523	0.000719491	2.990456	0.000587
Adipocytokine signaling pathway	0.000229	3.97E-05	0.00056871	8.91448E-05	2.485872	5.28E-05
Glycosaminoglycan degradation	0.000591	0.000192	0.001422714	0.000308326	2.407208	0.000906
N-glycan biosynthesis	0.000138	6.84E-05	0.000315045	3.57694E-05	2.288647	0.000885
Lipopolysaccharide biosynthesis proteins	0.002137	0.000495	0.004318864	0.000817478	2.021163	0.000924
Pores ion channels	0.001863	0.000362	0.003614931	0.000403516	1.940219	9.04E-05
Biotin metabolism	0.000737	0.00012	0.001397437	0.000283322	1.897122	0.001354
Lysosome	0.001063	0.000422	0.001944657	0.000416936	1.829121	0.010489
Membrane and intracellular structural molecules	0.003528	0.000487	0.006288046	0.000825152	1.782215	0.0002
Lipoic acid metabolism	0.000346	5.56E-05	0.000605686	4.30134E-05	1.749845	3.47E-05
Glycosphingolipid biosynthesis—globo series	0.000968	0.00025	0.001687631	0.00023645	1.743797	0.001584
Cell division	0.000391	0.000133	0.000680175	8.95898E-05	1.741208	0.003726
MAPK signaling pathway—yeast	0.000295	6.06E-05	0.00050885	5.64876E-05	1.725306	0.000418
Other glycan degradation	0.002301	0.000749	0.003676415	0.000702807	1.597939	0.01722
Geraniol degradation	0.000328	0.000101	0.000501312	9.54988E-05	1.5274	0.023563
β-Alanine metabolism	0.001292	0.000161	0.001947256	0.000148104	1.507311	0.000151
Epithelial cell signaling in *Helicobacter pylori* infection	0.000497	5.89E-05	0.000727172	0.000132278	1.462797	0.007475
Peroxisome	0.001235	0.00012	0.001796635	0.000203409	1.454585	0.000715
Folate biosynthesis	0.002742	0.000268	0.003975145	0.000334059	1.449917	0.0002
Restriction enzyme	0.001251	0.00021	0.00180323	0.000131348	1.440885	0.001072
Ubiquinone and other terpenoid-quinone biosynthesis	0.001934	0.000428	0.002779186	0.000355529	1.437162	0.009367
Vitamin B_6 metabolism	0.001409	0.000101	0.001952253	0.000105993	1.385308	3.36E-05
Prostate cancer	0.000285	6.63E-05	0.000390861	5.77957E-05	1.373171	0.027097
Pantothenate and CoA biosynthesis	0.004459	0.000455	0.005939913	0.000228313	1.332256	0.000186
Phenylalanine, tyrosine and tryptophan biosynthesis	0.004994	0.000746	0.006638512	0.000733047	1.329176	0.007904
Oxidative phosphorylation	0.009065	0.000724	0.012043546	0.000923537	1.32854	0.000467
Biosynthesis of vancomycin group antibiotics	0.000557	3.12E-05	0.000738663	5.77432E-05	1.325924	0.000263
Type I diabetes mellitus	0.000508	5.11E-05	0.000668144	2.83829E-05	1.315974	0.000277
Novobiocin biosynthesis	0.000895	0.000112	0.00115542	9.80467E-05	1.291529	0.004417
Citrate cycle (TCA cycle)	0.0054	0.000703	0.006966225	0.000461964	1.290068	0.003153
Butirosin and neomycin biosynthesis	0.000665	7.43E-05	0.0008484	1.0409E-05	1.275266	0.000603
Streptomycin biosynthesis	0.00279	0.000133	0.003490727	0.000125877	1.251237	2.68E-05
Polyketide sugar unit biosynthesis	0.001645	0.000198	0.002055614	0.000193223	1.249717	0.010475
Valine, leucine and isoleucine biosynthesis	0.005356	0.000533	0.006606412	0.000363613	1.233519	0.0025
Protein processing in endoplasmic reticulum	0.000669	8.18E-05	0.000822855	4.78304E-05	1.229143	0.006795
C5-Branched dibasic acid metabolism	0.002037	0.000182	0.002501844	0.000241029	1.228022	0.008865
PPAR signaling pathway	0.000767	5E-05	0.000934456	4.90901E-05	1.218818	0.000682
Alanine, aspartate, and glutamate metabolism	0.008727	0.000396	0.010503358	0.000446076	1.203543	0.00016
Biosynthesis and biodegradation of secondary metabolites	0.000459	6.44E-05	0.000551478	4.70822E-05	1.201522	0.032033
One carbon pool by folate	0.005687	0.000182	0.006791265	0.000112454	1.194251	2.91E-06
Histidine metabolism	0.005153	0.000806	0.006147774	0.000307342	1.193112	0.032689
Bacterial secretion system	0.005416	0.000606	0.006435057	0.000541889	1.188064	0.023087
Energy metabolism	0.007805	0.001144	0.009168472	0.000565065	1.174748	0.043794
Chaperones and folding catalysts	0.009367	0.000436	0.010994584	0.000375892	1.173817	0.000226
Carbon fixation pathways in prokaryotes	0.009048	0.000955	0.010612798	0.000520929	1.17298	0.012317
Prenyltransferases	0.00353	0.000364	0.004056902	0.000279875	1.149422	0.033191
RNA degradation	0.004528	0.000269	0.005196694	0.000131656	1.147767	0.001053
Glycine, serine and threonine metabolism	0.007509	0.00027	0.008559847	0.000104423	1.139965	3.94E-05
Zeatin biosynthesis	0.000469	2.93E-05	0.000531612	2.5473E-05	1.132638	0.007165
Lipid biosynthesis proteins	0.00567	0.000362	0.006368893	0.000312488	1.12328	0.011373
Arginine and proline metabolism	0.010138	0.000557	0.01129809	0.000713146	1.114462	0.020936
D-Glutamine and D-glutamate metabolism	0.001557	0.000129	0.001726176	5.46E-05	1.108855	0.026929
Protein export	0.005904	0.000285	0.006536028	0.000135405	1.107026	0.002049

(continued)

Supplemental Table IV. (continued).

Substance	*Vdr*$^{-/-}$ Cecal		*Vdr*$^{-/-}$ Fecal		Fold Change, Cecal To Fecal	*P*
	Mean	SD	Mean	SD		
Primary bile acid biosynthesis	0.000392	2.43E-05	0.000432578	1.90408E-05	1.103196	0.019017
Secondary bile acid biosynthesis	0.000392	2.43E-05	0.00043153	2.08464E-05	1.100525	0.024999
Translation factors	0.005488	0.000289	0.006037921	6.89646E-05	1.100239	0.003268
Carbon fixation in photosynthetic organisms	0.005572	0.00012	0.006094554	0.000214449	1.093874	0.001436
Methane metabolism	0.011181	0.00048	0.012170609	0.000722087	1.088538	0.034034
Ribosome biogenesis in eukaryotes	0.00047	2.77E-05	0.000501442	7.94075E-06	1.06736	0.039834
Lysine biosynthesis	0.007558	0.000181	0.008050973	0.000187745	1.065236	0.002868
Cell cycle—*Caulobacter*	0.005241	0.000224	0.005550626	0.000116164	1.059125	0.025213
Amino acid related enzymes	0.014394	0.000326	0.015237772	0.000180727	1.058627	0.000967
Pentose phosphate pathway	0.008979	0.000224	0.008276583	0.000403437	0.921804	0.009324
Propanoate metabolism	0.005791	0.000308	0.005312466	0.000187729	0.917341	0.017925
Function unknown	0.015325	0.000113	0.014005517	0.000749822	0.913921	0.00461
Bacterial toxins	0.001565	7.16E-05	0.001410092	3.77212E-05	0.900855	0.002654
Cytoskeleton proteins	0.003941	0.000377	0.003441119	0.000181533	0.873219	0.028409
Two-component system	0.014527	0.001149	0.012640043	0.001146434	0.870091	0.03163
Sulfur relay system	0.002594	0.00025	0.002231828	0.000241127	0.860244	0.047935
Glycerolipid metabolism	0.005011	0.000322	0.004269376	0.000216942	0.851942	0.002699
Chloroalkane and chloroalkene degradation	0.00248	0.000176	0.002079025	0.000328332	0.838247	0.042709
Carbohydrate metabolism	0.001436	0.000188	0.00117921	3.83699E-05	0.821197	0.017171
RNA transport	0.001807	0.000109	0.001478164	0.000142096	0.81786	0.003395
Benzoate degradation	0.003133	0.000193	0.002527748	0.000306766	0.806837	0.005776
Lipid metabolism	0.001722	7.44E-05	0.001341788	6.53639E-05	0.779121	2.62E-05
Transcription factors	0.018636	0.001075	0.01411196	0.001274457	0.757244	0.0003
ABC transporters	0.036675	0.002311	0.026996889	0.002562584	0.736107	0.00024
Phosphotransferase system (PTS)	0.00703	0.001328	0.005045259	0.00115418	0.717665	0.035667
Transporters	0.078468	0.007272	0.056242763	0.005554531	0.716758	0.000623
Retinol metabolism	0.00045	3.95E-05	0.000320739	8.94372E-05	0.712146	0.018004
Dioxin degradation	0.000823	0.000154	0.000568082	0.000128182	0.690357	0.021809
Metabolism of xenobiotics by cytochrome P-450	0.00045	3.97E-05	0.000299018	8.77652E-05	0.663984	0.007936
Xylene degradation	0.000656	8.99E-05	0.000430407	9.40074E-05	0.656556	0.004741
Drug metabolism—cytochrome P-450	0.000576	9.49E-05	0.000370909	0.000130777	0.644121	0.021965
Synthesis and degradation of ketone bodies	0.000651	0.000112	0.000401616	5.60109E-05	0.617388	0.002143
Biosynthesis of siderophore group nonribosomal peptides	0.000221	5.34E-05	0.000133863	2.26153E-05	0.606703	0.010143
Renal cell carcinoma	0.000218	6.57E-05	0.000112697	3.68862E-05	0.516682	0.014062
Sporulation	0.006536	0.002217	0.003210745	0.001126353	0.491213	0.017336
Electron transfer carriers	0.000621	0.000319	0.000236937	0.000171618	0.381528	0.045119
Prion diseases	0.000144	5.63E-05	4.64253E-05	1.792E-05	0.323005	0.006209